SUPPLEMENTARY APPENDIX

Sphingolipid dysregulation due to lack of functional KDSR impairs proplatelet formation causing thrombocytopenia

Tadbir K. Bariana,[1.2.3,4] Veerle Labarque,[5] Jessica Heremans, [5] Chantal Thys,[4,5] Mara De Reys,[5] Daniel Greene,[3,4,6,7] Benjamin Jenkins,[8] Luigi Grassi,[3,4,6,7] Denis Seyres,[3,4,6,7] Frances Burden,[3,4,6] Deborah Whitehorn,[3,4,6,] Olga Shamardina,[3,4,6] Sofia Papadia,[3,4,6] Keith Gomez,[1,2,4] NIHR BioResource,[4] Chris Van Geet,[4,5] Albert Koulman,[8] Willem H. Ouwehand,[3,4,6,9,10] Cedric Ghevaert,[3,6,9] Mattia Frontini,[3,4,6,9] Ernest Turro[3,4,6,7] and Kathleen Freson[4,5]

[1]Department of Haematology, University College London, UK; [2]The Katharine Dormandy Haemophilia Centre and Thrombosis Unit, Royal Free London NHS Foundation Trust, UK; [3]Department of Haematology, University of Cambridge, Cambridge Biomedical Campus, UK; [4]NIHR BioResource, Cambridge University Hospitals, Cambridge Biomedical Campus, UK; [5]Department of Cardiovascular Sciences, Center for Molecular and Vascular Biology, University of Leuven, Belgium; [6]NHS Blood and Transplant, Cambridge Biomedical Campus, UK; [7]Medical Research Council Biostatistics Unit, Cambridge Institute of Public Health, Cambridge Biomedical Campus, UK; [8]NIHR Biomedical Research Centre Core Metabolomics and Lipidomics Laboratory, University of Cambridge, Cambridge Biomedical Campus, UK; [9]British Heart Foundation Centre of Excellence, Division of Cardiovascular Medicine, Cambridge University Hospitals, Cambridge Biomedical Campus, UK and [10]Wellcome Sanger Institute, Wellcome Genome Campus, Hinxton, Cambridge, UK

 doi:10.3324/haematol. 2018.204784

Received: August 17, 2018.

Accepted: November 19, 2018.

Pre-published: November 22, 2018.

Correspondence: KATHLEEN FREESON kathleen.freson@med.kuleuven.be

Supplemental Materials

Supplemental Methods

Recruitment and sequencing

Genetic variants were identified from whole genome sequencing (WGS) data using Isaac (Illumina Inc.) or as described previously for whole exome sequencing.[1] Clinical and laboratory phenotypes were recorded in raw form and as Human Phenotype Ontology (HPO) terms along with pedigree data.[1] The propositus' genetic and phenotypic data were analyzed as part of a dataset of from 9,472 study participants that have undergone genetic analysis, which includes 1,472 cases with unexplained BPDs.

Platelet imaging

Platelet imaging was performed using a structured illumination microscope (SIM, Elyra S.1, Zeiss, Heidelberg, DE). Images were analyzed with ZEN Black (Carl Zeiss Inc., Oberkochen, DE) and ImageJ software (National Institutes of Health (NIH), Bethesda, MD).[2] Raw 3D SIM images were processed to super-resolution SIM using ZEN Black software, followed by maximum intensity projection as previously described.[3]

Metabolic profiling

In the targeted sphingolipid profiling protocol, for the identification of KDS we used a Thermo Scientific Q-Exactive Orbitrap (ThermoFisher Scientific, Hemel Hempstead, UK) set up to fragment the 300.3 ion (±2 m/z) using a relative collision energy of 30. The KDS standard used was purchased from Matreya LLC (Cat. no. 1876, State College, PA). All samples were snap frozen in dry ice and stored at -80^{0}C until analysed. Zebrafish lysates for sphingolipid profiling were prepared as for immunoblot analysis, using 20 embryos per condition, in triplicate, isolated at 72 hours post fertilisation [hpf].[4]

Stem cell differentiation assays

$CD34^+$ hematopoietic stem cells (HSC) isolated from bone marrow aspirates from the propositus (at 5 years of age) and an unrelated control, and from peripheral blood from the propositus (at 8·5 years of age), his affected sister (at 5 months of age) and an unrelated control were stored in liquid nitrogen. The recovered (differentiation day 0) CD34+ HSCs were cultured in StemSpan SFEM medium with StemSpan CC100 ensuring strong expansion of HSC for 3 days (Stem Cell Technologies, Vancouver, CA).

The expanded bone marrow derived HSC were used to perform colony assays for MK (CFU-MK) and granulocytes, erythrocytes, monocytes, and MK (GEMM; CFU-GEMM) as described previously.[4, 5] These were performed in quintuple for MegaCult-C 04973 (MK) and triplicate for MethoCult 04964 (GEMM, StemCell Technologies, Vancouver, CA). MK (after Giemsa staining) and GEMM (without staining) colonies were counted by two independent operators using a Zeiss Axiovert 200M microscope (Carl Zeiss Inc.) or light microscope (Leica DM RBE, Wetzlar, DE), respectively. Colonies from GEMM plates were further analysed by flow cytometry using FITC-labelled mouse antibodies against glycophorin A (CD235a; BD Biosciences, San Jose, CA) and PE-labelled mouse antibodies against CD45 (Clone T29/33; Dako, Glostrup, DK).

Liquid MK cultures were derived from bone marrow- and peripheral blood- derived HSC at day 3 of differentiation by incubation with 50ng/ml thrombopoietin (TPO), 25ng/ml stem cell factor, and 10ng/ml

interleukin 1β (Peprotech, Rocky Hill, NJ,). MK were analysed by flow cytometry on total differentiation day 7 with FITC-labelled antibodies against CD41 and CD42 (BD Biosciences) and on total differentiation day 11 for proplatelet formation and immunostaining of cytoskeletal proteins F-actin, phalloidin-rhodamine (Sigma, St Louis, MO), and anti-tubulin (ThermoFisher Scientific), and δ-granule and lysosome marker CD63 (Santa Cruz, Dallas, TX).[5, 6] For immunostaining MK were seeded for 4 hours on fibrinogen-coated coverslips and stained cells were photographed at 63x magnification with a confocal microscope (AxioObserver.Z1, Zeiss, Heidelberg, DE). MK cell size was determined by F-actin staining and images were analyzed with ImageJ software (NIH[2]). Three random control images were used to optimize parameters and MK were excluded if the ploidy was unclear following F-actin staining, as described.[7]

Statistical analysis of MK size following immunostaining

Using the lmer function from the R package lme4 a linear mixed effects model was fitted to the log of MK cell size:

$$y_{ijkl} = \alpha + \beta p_{ijk} + \gamma s_i + \xi f_j + \delta p_{ijk} s_i + \eta_i + \epsilon_{ijkl}$$

$$\eta_i \sim N(0, \sigma_\eta^2)$$

$$\epsilon_{ijkl} \sim N(0, \sigma_\epsilon^2)$$

where y_{ijkl} corresponds to the *k*th observation for individual $i \in \{1,2,3,4\}$ obtained as part of experiment $j \in \{1,2\}$. The covariate p_{ijk} is equal to 0, 1 or 2 depending on whether the ploidy was 1, 2 or between 4 and 8, respectively. The covariate s_i equals 1 if individual *i* is a case and 0 otherwise. The covariate f_j equals 1 if *j*=2 and 0 if *j*=1. The interaction term δ captures the difference in the ploidy-dependent slope between cases and controls. Inter-individual variation is modelled with normally distributed random effects (η_i).

The regression coefficients $\hat{\alpha}, \hat{\beta}, \hat{\gamma}, \hat{\xi}, \hat{\delta}$ were estimated by maximum likelihood and associated *p*-values were computed by a likelihood ratio test and were as follows:

MK cell size:

$\hat{\alpha} = 7.78075$

$\hat{\beta} = 0.35496$

$\hat{\gamma} = -0.42443$ $p = 0.01473$

$\hat{\xi} = -0.05632$

$\hat{\delta} = 0.07197$ $p = 0.2641$

iPSC derivation

iPSC were prepared by the Cambridge Biomedical Research Centre iPSC core laboratory from fibroblasts isolated from a 2mm skin biopsy of the propositus' upper arm. Fibroblasts were reprogrammed following the protocol of Yamanaka and colleagues[8, 9] by overexpression of transcription factors OCT4, SOX2, KLF4, and c-MYC using the CytoTune™-iPS 2·0 Sendai Reprogramming Kit (Invitrogen) followed by culture on mouse embryonic fibroblast feeder cells in chemically defined media. Following establishment of iPSC colonies, approximately one month after reprogramming, clones were picked, passaged to feeder-free conditions, and validated. iPSC were cultured feeder- and antibiotic- free in Essential 8 medium (ThermoFisher Scientific).

Lentiviral particle production, transduction and selection

Replication-deficient lentiviral vector particles were produced by transient co-transfection of HEK 293T cells with the rescue or empty vector and a 2nd generation packaging system consisting of psPAX2 and pCMV-VSV-

G (Addgene #12260, #8454). Viral particles were concentrated by the LentiX-concentrator system (Clontech). Transduction was performed in iPSC at MOI 2, in the presence of protamine sulphate 10μg/ml (Sigma) and was followed by plate centrifugation at 2500 rpm for 45 minutes at 37^{0}C. Cells carrying the rescue or empty vector were selected after 72 hours using 0·1μg/ml puromycin (Sigma).

Forward programming to MK (iMK)

Passage to single iPSC was obtained using TrypLE (ThermoFisher Scientific) followed by culture in Essential 8 media containing 10μM ROCK inhibitor (Sigma) for 24 hours prior to lentiviral transduction with *FLI1, GATA1,* and *TAL1* using a protocol for generating MK described by Moreau *et al.*[10] The MK obtained by this protocol (named iMK hereafter) were defined at day 20 post-transduction by absence of staining with 1μg/ml DAPI (Sigma; at this concentration live iMK are impermeant to DAPI) and dual staining with anti-CD41a-APC and anti-CD42b-PE (1:100, cat. 559777 and 1:1000, cat. 555473, respectively, BD Biosciences) on the Beckman Coulter Gallios Cytometer. Cytometry results were analysed using Kaluza Analysis v.1.5a (Beckman Coulter).

Proplatelet assay

iMK were placed at a concentration of 0·5x10^6/ml in CellGro medium (CellGenix) for seeding on sterile glass coverslips coated with 200μg/ml fibrinogen (Sigma**)** in phosphate-buffered saline (PBS). Cells were fixed in 1% paraformaldehyde at 4 hours or 24 hours after seeding. Cells were quenched with 50μM ammonium chloride and permeabilized with 0·1% saponin, 0·2% gelatin, and 0·02% azide (Sigma) in PBS. Staining was performed with antibody against α-tubulin (1:250, cat.T5168, Sigma), 1μg/ml DAPI (Sigma), and goat anti-mouse Alexa Fluor 488 antibody (1:1000, cat. A21121, ThermoFisher Scientific). Cells were examined within 48 hours using a Leica DMi8 fluorescent microscope and images were analysed using FIJI software.[2] Five to ten representative fields were examined to ensure at least 100 iMK were observed for each experimental condition. Proplatelets were defined as clear projections from the main cell body with approximately parallel sides to the shaft. Results were compared using the paired, two-tailed Student's *t*-test.

RNA sequencing

1 x 10^5 iMK were stored in 500 μl Trizol reagent (ThermoFisher Scientific) at -80^{0}C. RNA was recovered for sequencing (RNA-seq) with the Direct-zol RNA MiniPrep kit (Zymo). RNA was quantified using the Qubit RNA HS Assay kit (ThermoFisher Scientific) and its quality was confirmed using the Agilent RNA 6000 Pico kit on the Agilent 2100 Bioanalyzer. cDNA libraries were prepared using the KAPA Stranded RNA-Seq Kit with Riboerase (Roche) and Agencourt AMPure XP beads (Beckman Coulter) for purification. Libraries were quantified by RT-qPCR with the KAPA Library Quantification Kit (Roche). Libraries were sequenced at the Cancer Research UK Cambridge Institute Genomics Core) on a HiSeq4000 (Illumina Inc.) using 150bp read length paired-end sequencing. Sequences were aligned with STAR[11] and read counts were obtained using featureCounts[12] with respect to Ensembl v.70 of reference genome build GRCh37. Expression of transcripts and genes was quantified using MMSEQ and differential expression was assessed using MMDIFF[13, 14]. The prior probability of differential expression was set to 0·1 and a posterior probability >0·5 was used to declare a transcript being differentially expressed.

Supplemental Table 1: Clinical data

(A) Serial blood results for propositus and pedigree members. Abnormal results are shown in bold. Spontaneous improvements in both platelet count and hemoglobin level were observed in the propositus, though the improvement in platelet count was not sustained. The affected sibling's platelet count and haemoglobin values have been decreasing since birth.

	WBC ($x10^9$/L)	**Neutrophils ($x10^9$/L)**	**Erythrocytes ($x10^6$/L)**	**Reticulocytes ($x10^9$/L)**	**Immature reticulocyte fraction (%)**	**Hemoglobin (g/dL)**	**Platelets ($x10^9$/L)**
Control values Neonates (<6 months)	*5.5-21*	*1.5-10*	*3.9-6.3*	*20-100*	*5-21*	*13.5-21.5*	*150-550*
Control values Adults (> 7 year)	*4.5-13.5*	*1.5-8.5*	*4-5.2*	*20-100*	*5-21*	*11.5-15.5*	*150-450*
Control values Children	*5.5-15.5*	*1.5-8.5*	*3.9-5.3*	*20-100*	*5-21*	*11.5-13.5*	*150-550*
Father	5.9	3.21	4.88	ND	ND	15.5	258
Mother	5.22	2.94	4.25	ND	ND	12.8	415
Healthy brother, 4 years	5.04	1.59	3.94	ND	ND	11.5	521
Propositus, 4 months	11.3	5.9	**3.8**	**19**	ND	**10.6**	**65**
Propositus, 1 years	8.85	3.8	3.91	45	18.2	**10.0**	**65**
Propositus, 2 years	10.98	4.7	3.94	43	**25.4**	**10.2**	**64**
Propositus, 3 years	10.22	3.3	**3.78**	39	**27.2**	**10.3**	**60**
Propositus, 4 years	7.84	3.9	**3.41**	27	**39.3**	**9.1**	**9**
Propositus, 5 years	14.53	9.7	**3.69**	56	**32**	**10.7**	**41**
Propositus, 6 years	7.61	2.9	**3.77**	**14**	**22.2**	**10.6**	**15**
Propositus, 8 years	7.06	3	4.67	25	7.8	13.6	**77**
Propositus, 8.5 years	9.49	4.4	4.24	37	9.7	12.5	152
Propositus, 9 years	7.89	3.9	4.2	36	10.6	12.5	**132**
Propositus, 9.5 years	9.97	5.6	4.72	40	10.4	13.4	**113**
Affected Sister, 1 week	11.64	3.4	5.73	25	16.1	19.1	**73**
Affected Sister, 5 months	9.34	2.2	**3.33**	45	**24.7**	**8.6**	**148**
Affected Sister, 7 months	10.15	3.8	**3.2**	34	**22.2**	**7.8**	**124**
Affected Sister, 9 months	13.18	5.5	**3.2**	72	**32.1**	**7.7**	**107**
Affected Sister, 1 year	14.58	4.1	**2.67**	76	**41.6**	**6.3**	**24**

(B) Serial assessments of peripheral blood films and bone marrow biopsies in the propositus.

	Peripheral blood smears	**Bone marrow biopsy**	**Bone marrow genetics**
II:2 (Propositus) 4 years	White blood cells normal, mild normocytic normochromic anemia with mild aniso-poikilocytosis and severe thrombocytopenia.	Erythrophagocytosis. Dysplastic megakaryocytes that are located in clusters. Normal lymphoid lineage with granulocytes. Myelofibrosis grade 2 reticulin staining.	Negative: BCR-ABL, FISH (monosomy 7), JAK2, CALR and MPL, chromosomal breakage
II:2 (Propositus) 5 years	Mild monocytosis and neutrophilia , mild normocytic normochromic anemia with anisopoikilocytosis and obvious thrombocytopenia	Left-shifted myeloid lineage. Increased numbers of dysplastic megakaryocytes. Erythroid lineage difficult to study due to insufficient numbers. Myelofibrosis grade 3. Cellularity 90%, myeloid/erythroid: 4/1.	
II:2 (Propositus) 8 years	Mild poikilocytosis and thrombocytopenia.	Normal cellularity 70-80%. Normocellular but hyperplastic and left-shifted myeloid lineage. Prominent hyperplastic megakaryocyte lineage with strong cluster formation on LAT staining. Megakaryocyte dysplasia with both hyperlobulated and small hypolobulated, hyperchromic cells. Normocellular erythroid lineage without dysplasia. Myelofibrosis grade 3. Mason trichrome staining of bone marrow showed mature collagen fibers (grade 3).	Negative: NGS panel test TruSight Myeloid Sequencing (Illumina) with coverage of 500x. FISH with normal karyotype.

(C) Platelet light transmission aggregometry studies.

The propositus had normal aggregation responses for ristocetin (105%), arachidonic acid (95%), U46619 (111%), collagen at 2 μg/ml (70%) and ADP at 5 μM (97%). Only the response to low dose of collagen was mildly reduced.

	Propositus*	**Two unrelated healthy controls***
Amplitude for Horm collagen 1μg/ml	25%	63 and 66%
Amplitude for ADP 2.5 μM	52%	48 and 28%

*All aggregations were performed using platelet-rich plasma at $90x10^3$ platelets/μL.

Supplemental Table 2

Ion counts from Metabolon analysis of plasma sphingolipids from the propositus, healthy brother, parents, and 496 unrelated controls.

3-ketosphinganine (KDS) was detectable in only the propositus. Downstream metabolites were not reduced, and the enzymatic product of KDSR dihydrosphingosine (DHS) was in fact unexpectedly high. NF, not found

	Propositus	Healthy brother	Mother	Father	Median (controls)	S.D (controls)
KDS	8.5 E5	NF	NF	NF	NF	NF
DHS	3.6 E5	NF	NF	NF	6.7 E4	3.2 E4
Dihydroceramide	6.3 E5	2.5 E5	3.3 E5	2.6 E5	3.1 E5	1.8 E5
Sphinganine-1-phosphate	6.7 E5	4.0 E5	4.6 E5	3.4 E5	3.9 E5	1.4 E5
Ceramide	3.5 E6	2.8 E6	3.6 E6	2.9 E6	2.8 E6	7.9 E6
Sphingosine	1.8 E5	9.5 E4	1.0 E5	6.2 E4	1.5 E5	8.3 E4
Sphingosine 1-phosphate	3.4 E6	2.7 E6	3.1 E6	2.3 E6	2.6 E6	6.2 E5
Total sphingomyelins	1.3 E9	1.2 E9	1.2 E9	1.3 E9	1.2 E9	1.8 E8
Total glycosphingolipids	1.2 E7	1.2 E7	8.9 E7	1.2 E7	1.0 E7	2.6 E6
Phosphoethanolamine	1.6 E6	1.7 E6	1.1 E6	8.0 E5	1.6 E6	6.1 E5

Supplemental Table 3

Ion counts from targeted sphingolipid analysis by LC-MS

(A) Plasma sphingolipid analysis by LC-MS. Metabolites downstream of KDSR were not reduced in affected individuals (propositus, affected sister) compared with unaffected individuals (healthy brother, parents and controls). DHS, sphingosine and S1P are not measurable by this method. Differences were analyzed using the paired, two-tailed Student's *t*-test, using $p<0.05$ for significance.

Plasma	Propositus	Affected Sister	Healthy Brother	Mother	Father	Control 1	Control 2	*p*
Dihydroceramides	3.78E-3	6.06E-3	3.90E-3	3.21E-3	2.60E-3	2.34E-3	8.46E-3	0.52
Ceramides	2.34E-2	8.70E-3	7.21E-3	6.48E-3	8.66E-3	5.64E-3	1.37E-2	0.5
Glycosphingolipids	1.78E-3	1.05E-3	1.69E-3	1.85E-3	1.98E-3	1.64E-3	4.04E-3	0.56
Sphingomyelins	11.7	5.26	9.31	9.01	11.3	4.17	11.5	0.74

(B) Analysis of zebrafish protein lysates by LC-MS. Metabolites downstream of Kdsr were not significantly different between *kdsr*-ATG morpholino targeted fish (800μM) and controls. Differences were analyzed using the paired, two-tailed *t*-test, using $p<0.05$ for significance.

Zebrafish protein lysate	Control 1	Control 2	Control 3	*kdsr*-ATG 1	*kdsr*-ATG 2	*kdsr*-ATG 3	*p*
Dihydroceramides	1.02 E3	2.31 E3	8.31 E4	5.98 E4	3.26 E4	5.23 E4	0.16
Ceramides	3.67 E3	9.43 E3	3.07 E3	3.43 E3	1.46 E3	3.82 E3	0.33
Glycosphingolipids	5.11 E5	0.00	4.40 E5	3.26 E5	5.28 E5	1.01 E4	0.19
Sphingomyelins	2.05	2.06	2.02	2.06	1.64	2.34	0.91

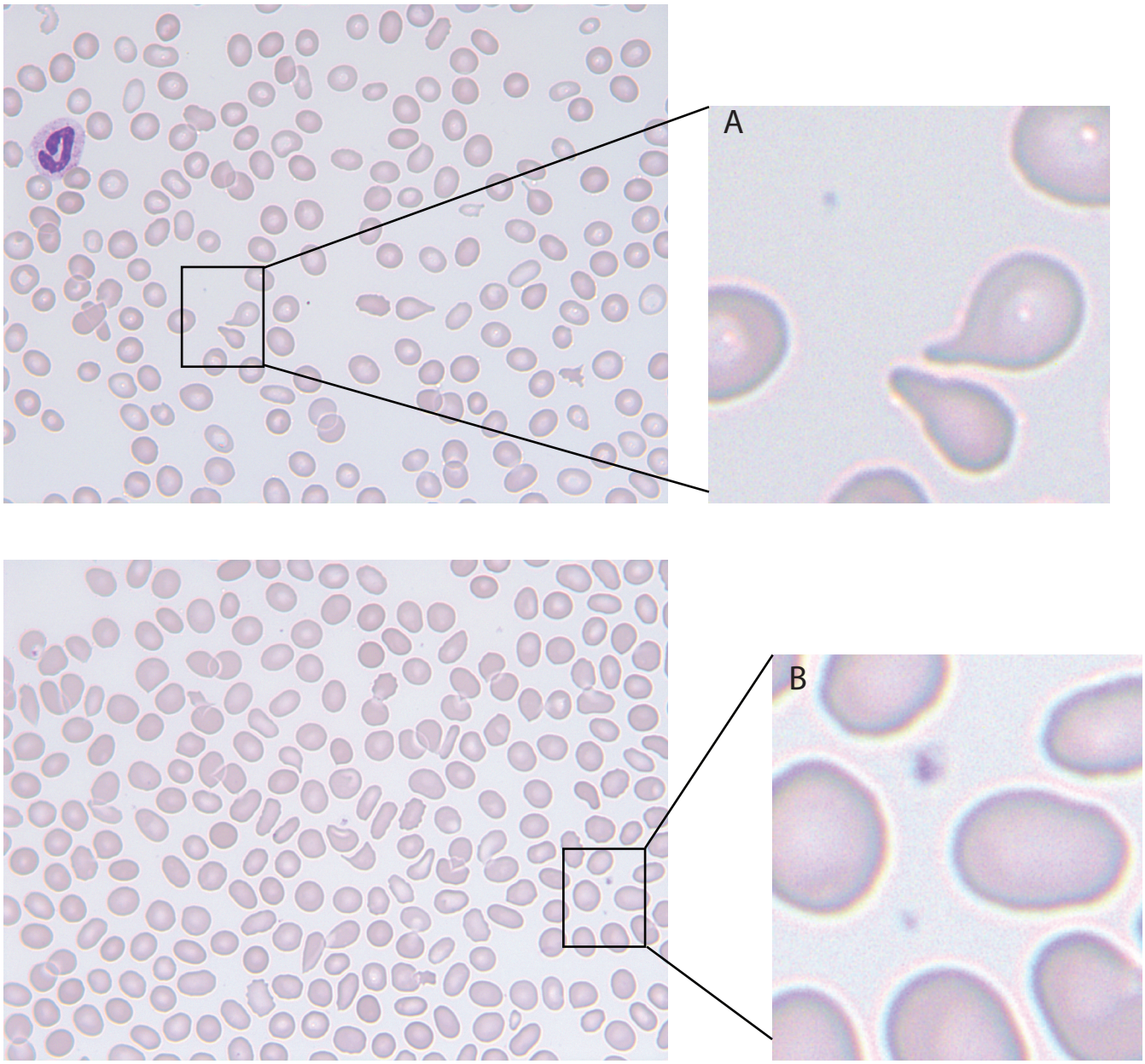

Supplemental Figure 1
Peripheral blood smears from the propositus taken at 6 years of age
Dysmorphic erythrocytes with poikilocytosis including (A) tear drop cells and (B) thrombocytopenia with platelets of normal volume are shown (magnification x100).

A

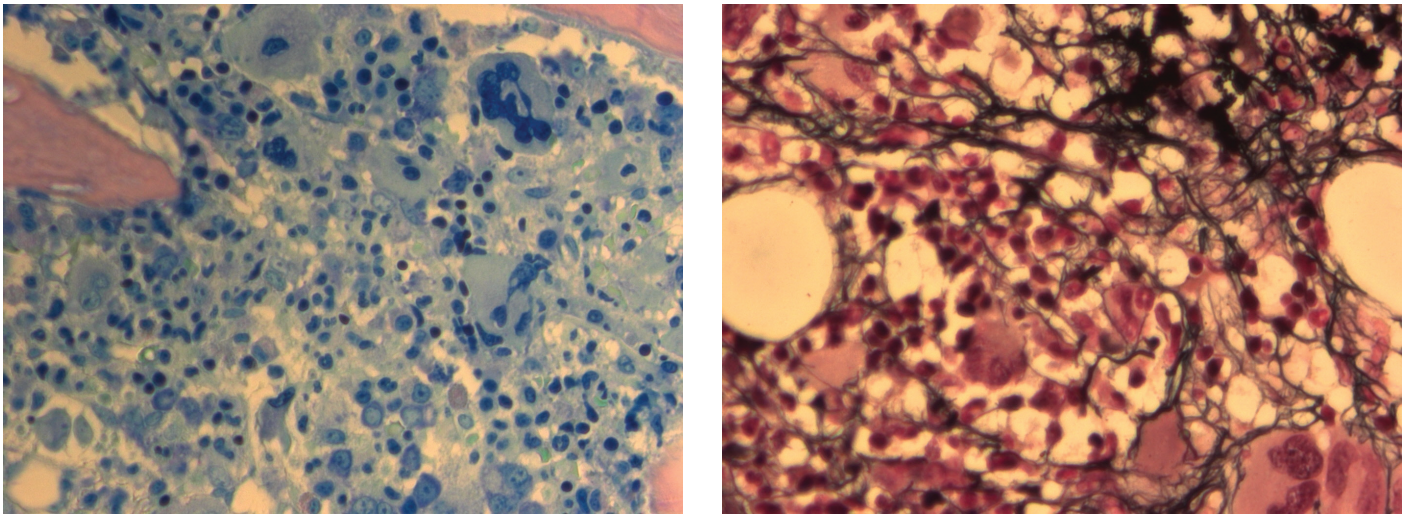

B

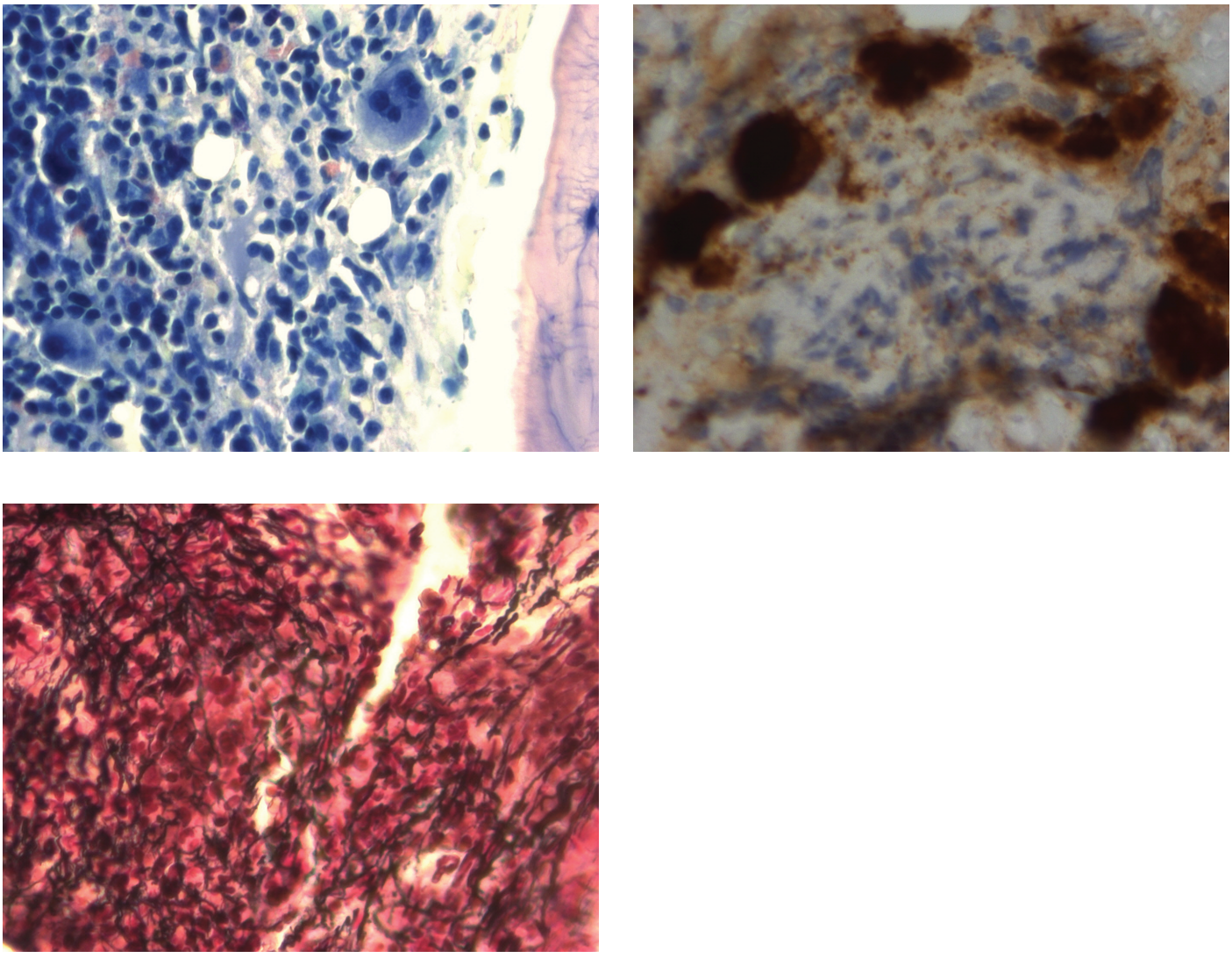

Supplemental Figure 2
Bone marrow (BM) biopsies from the propositus
(A) BM biopsy at 4 years of age. Left: Dysplastic megakaryocytes (MK) forming unusually large clusters. Right: Fibrosis with reticulin staining. (B) BM biopsy at 8 years of age. Left and right upper: Dysplastic MK in clusters. Left lower: Marrow fibrosis with strong stromal reticulin staining (magnification x40).

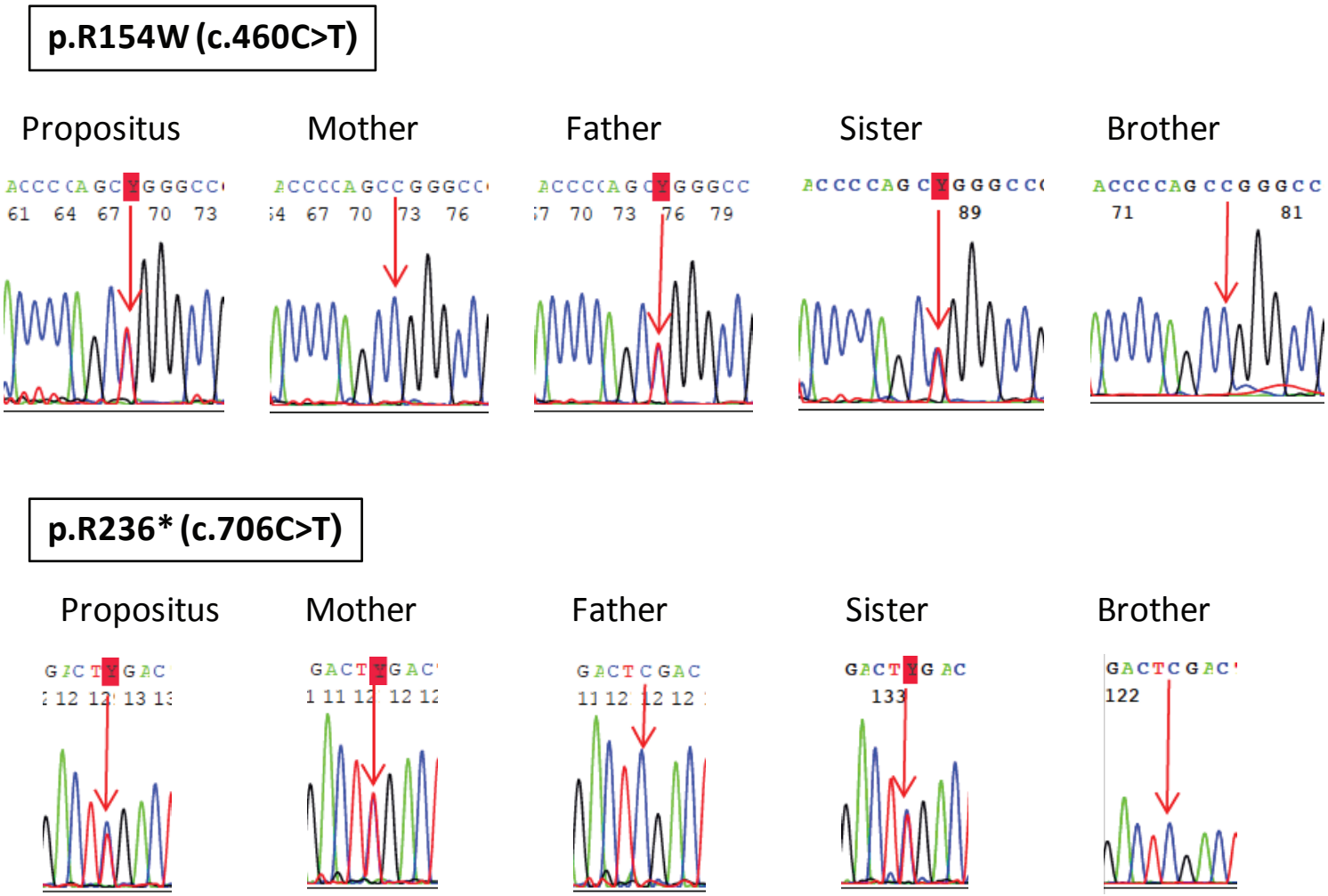

Supplemental Figure 3
Sanger sequencing confirms putative pathogenic *KDSR* variants
Two rare variants (18:61006104 G>A and 18:61018270 G>A) were confirmed by Sanger sequencing in the proband and his affected sister. The healthy brother carried the major allele for both variants.

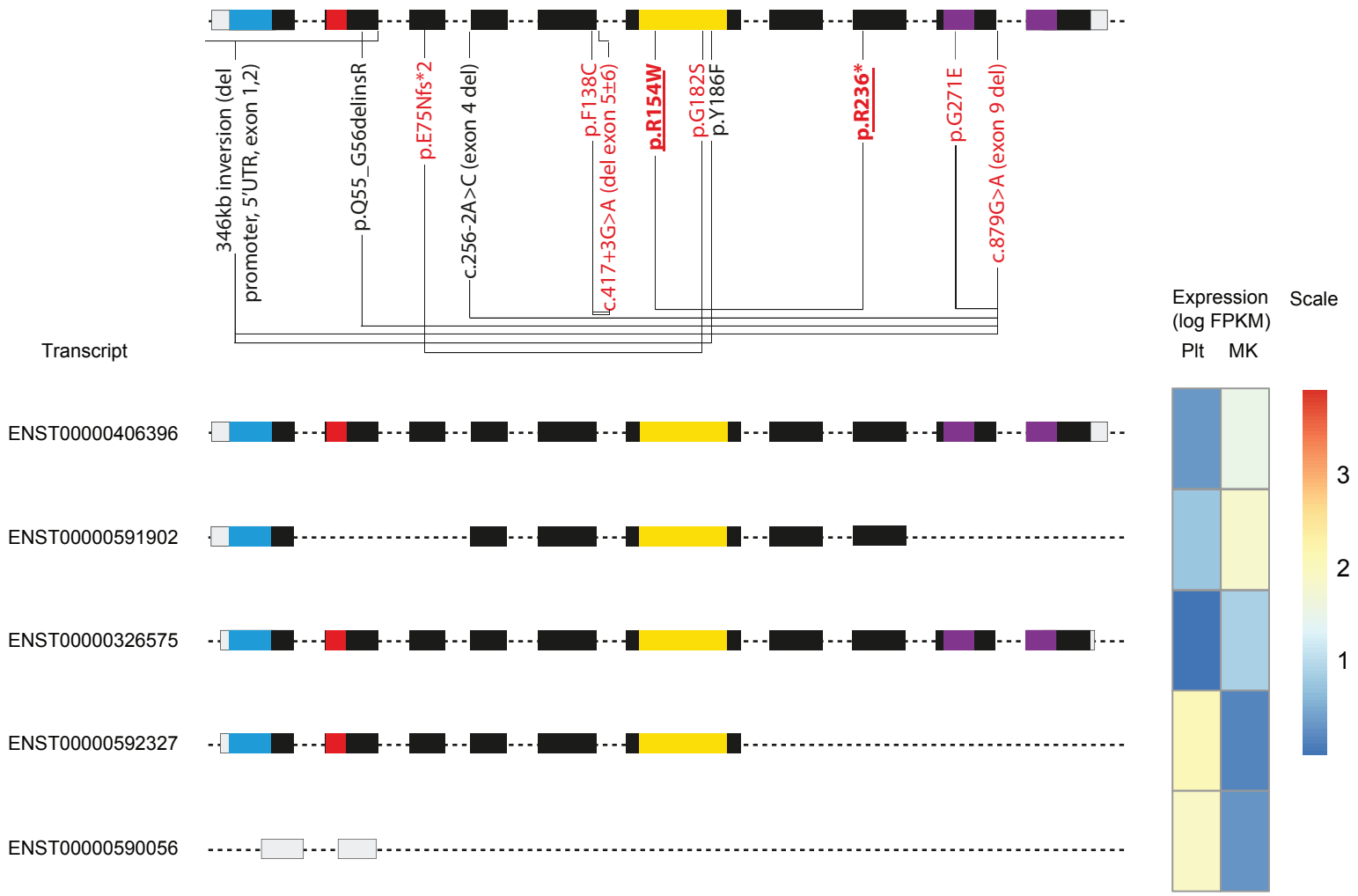

Supplemental Figure 4

Heatmap of *KDSR* transcripts in MK and platelets (Plt)

Transcripts present at >0·5 log FPKM (fragments per kilobase of transcript per million mapped reads) are shown and schematically represented. Key structural elements and variant annotation are as defined in Figure 1. The variants present in the affected siblings are highlighted in bold, and are present in the major transcripts present in MK (ENST00000406396, ENST00000591902) but not platelets (ENST00000592327, ENST00000590056, http://blueprint.haem.cam.ac.uk).[8] This is in keeping with previous reports that de novo sphingolipid synthesis plays a minimal role in mature platelets.[9]

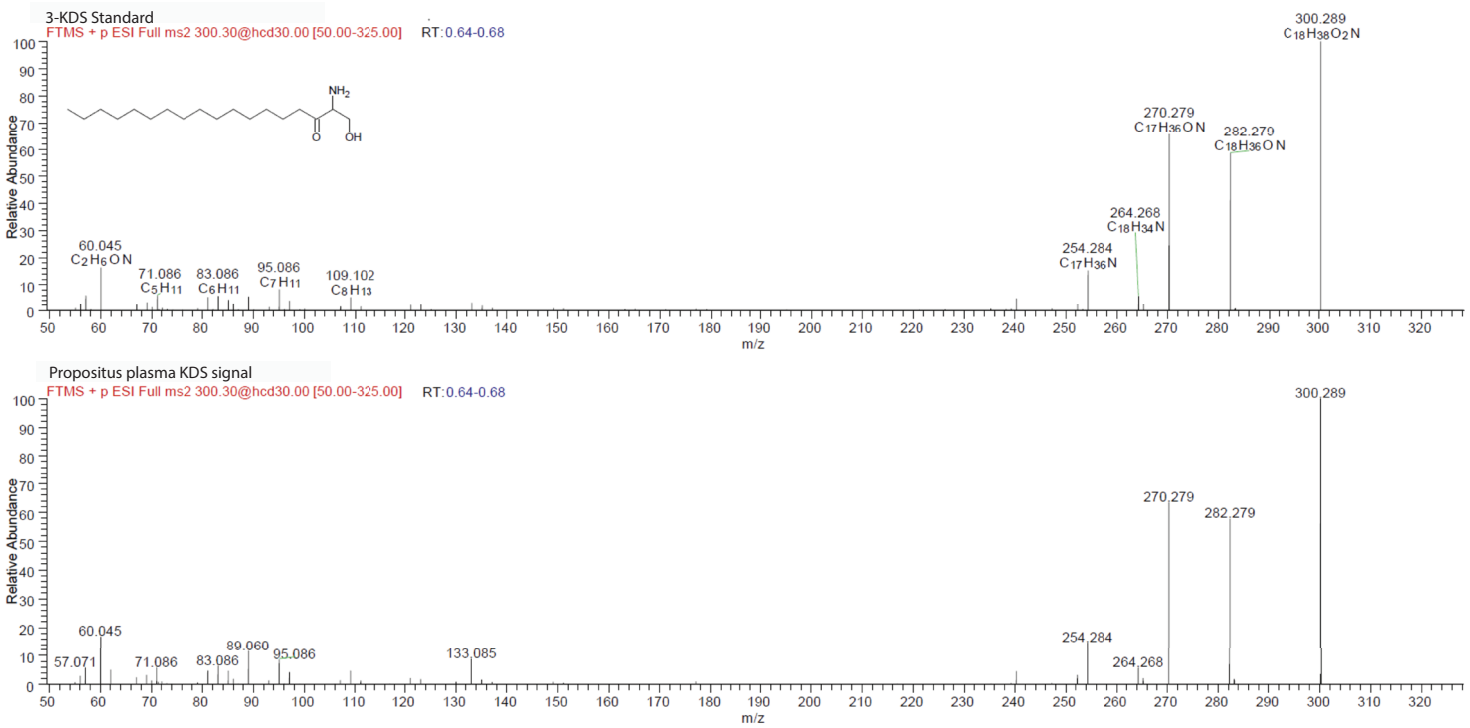

Supplemental Figure 5

Mass spectrum of 3-KDS in propositus and standard

An LC-MS platform was used to confirm the metabolic phenotype in the propositus and affected sister. The MS2 spectrum is shown for the 3-KDS biochemical standard and the propositus, showing conformity of peaks. FTMS, Fourier transformation mass spectrometry; +pESI, positive mode electrospray ionisation; HCD, higher energy collisional dissociation. Set at the specific fragmentation of ion 300·3 m/z by HCD at a relative energy of 30%, obtaining data from the range 50 to 325 m/z.

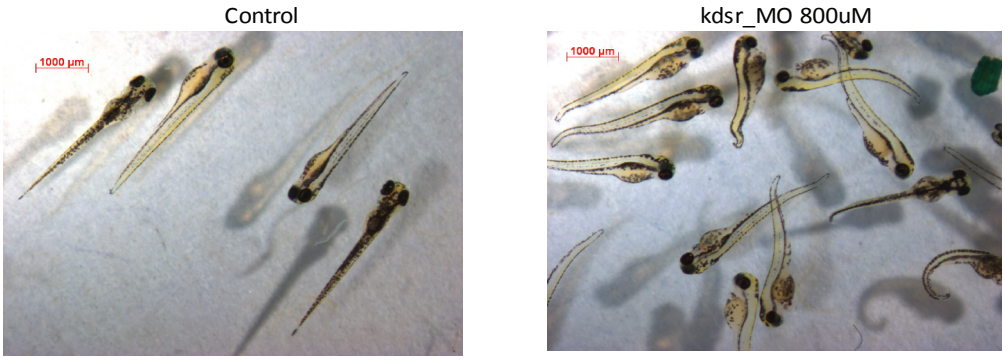

Supplemental Figure 6
Zebrafish experiments
Tg(cd41:EGF) embryos were injected with a kdsr ATG-MO (1000 µM) or with buffer (control). At 72 hpf most embryos developed curled tails but no other dysmorphisms.

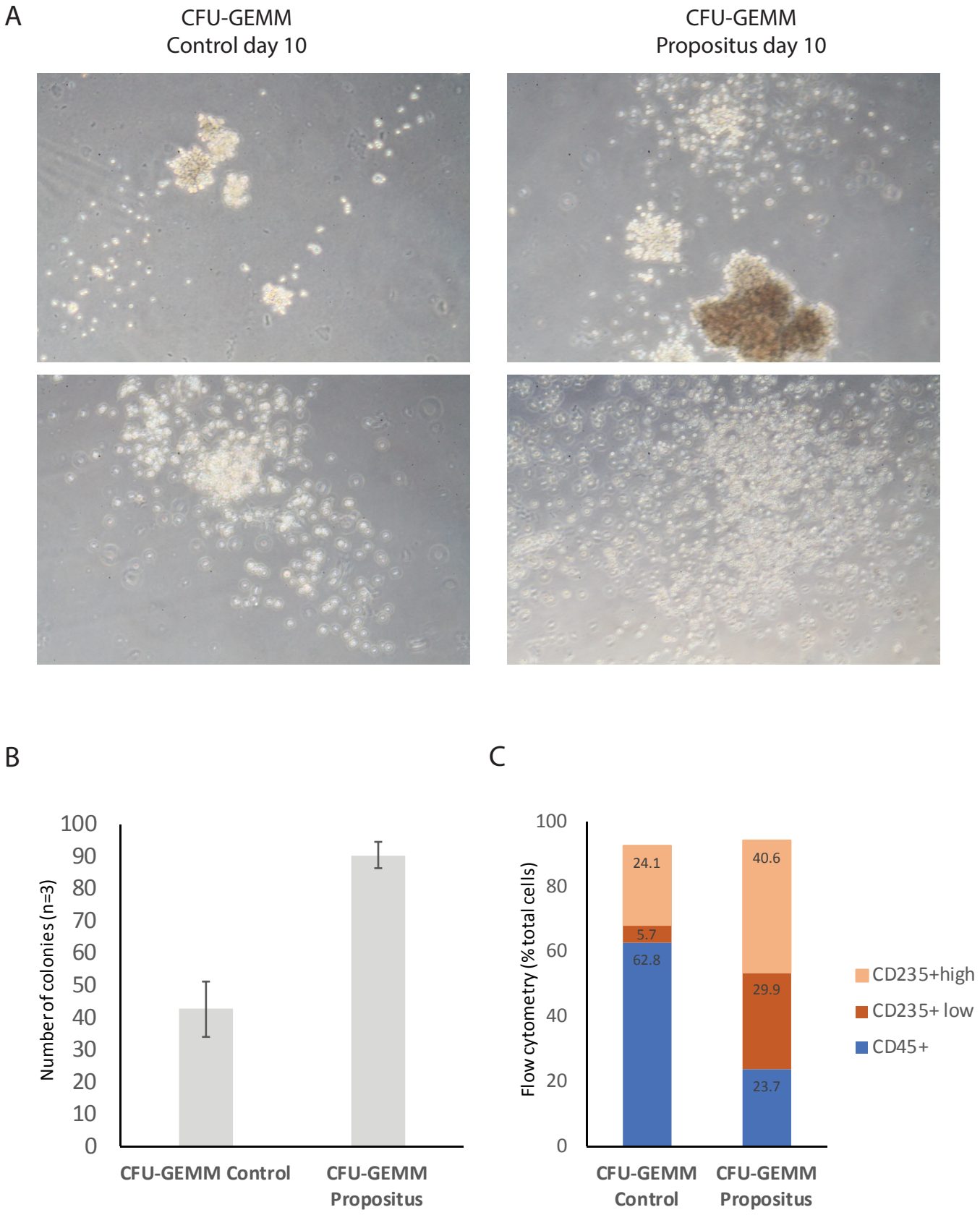

Supplemental Figure 7
Myeloid stem cell differentiation assays from propositus at 5 years of age
(A, B) Representative images of CFU-GEMM colonies counted at day 10 of differentiation of CD34+ bone-marrow HSC. There was a higher number and increased density of colonies for the propositus compared with controls. Means and standard deviations of three experiments are shown. (C) Flow cytometry analysis following staining with anti-CD45 and anti-CD235 antibodies to stain the myeloid and erythroid lineage, respectively. The proportion of myeloid leukocytes was higher in control cultures, whilst cultures from the propositus were enriched for erythroid progenitors.

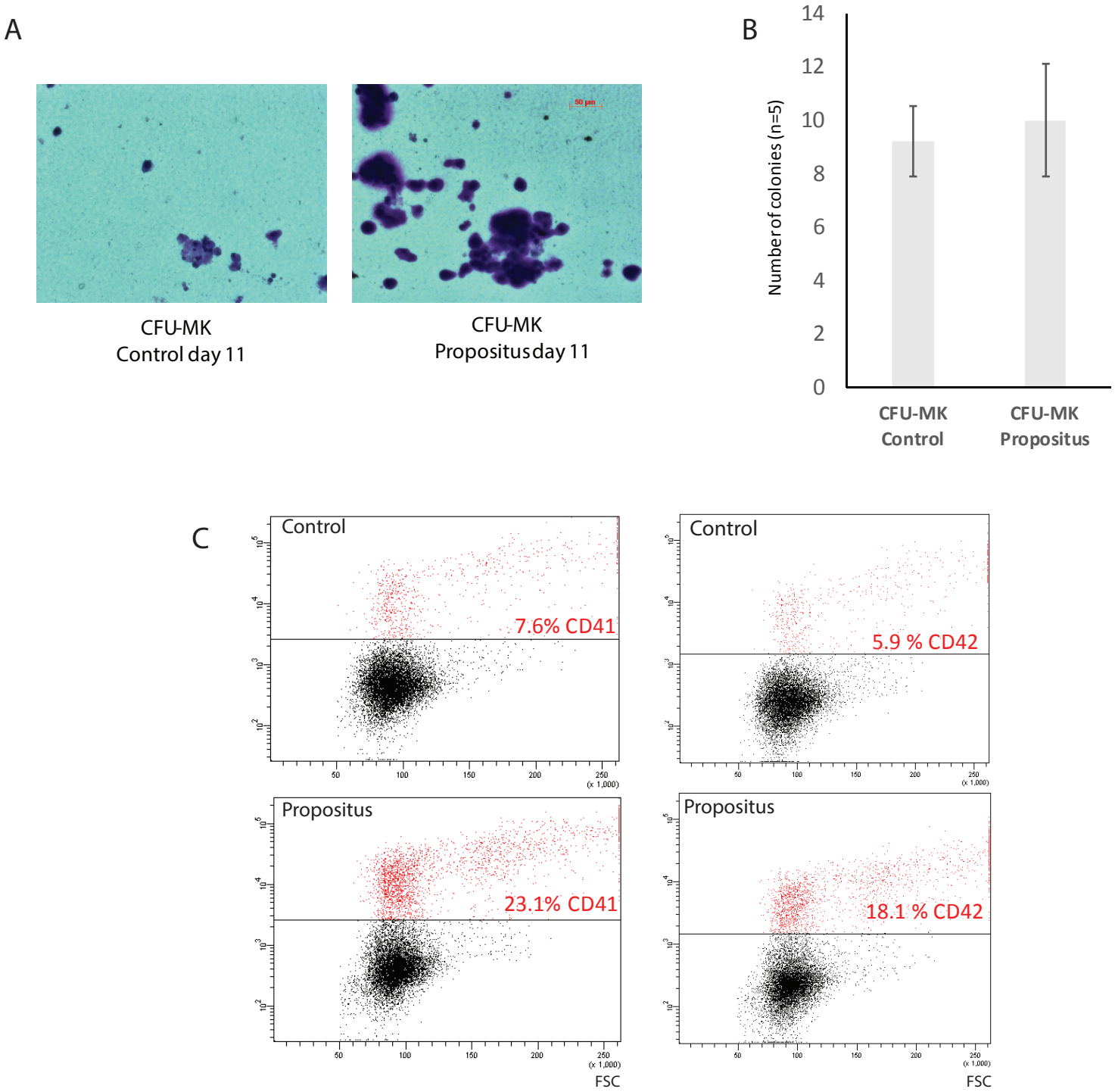

Supplemental Figure 8
Megakaryocyte colony assays
(A) MegaCult cultures. Representative images of CFU-MK colonies at day 11 of differentiation of CD34+ bone-marrow HSC. We observed an increased density of colonies for the propositus compared with controls. (B) However the total number of MK colonies was comparable between conditions. Means and standard deviations of 5 experiments are shown. (C) Liquid MK cultures were analysed at day 7 of differentiation using flow cytometry. A higher number of cells expressed mature MK markers CD41 and CD42 in cultures derived from the propositus compared with controls. FSC, forward scatter.

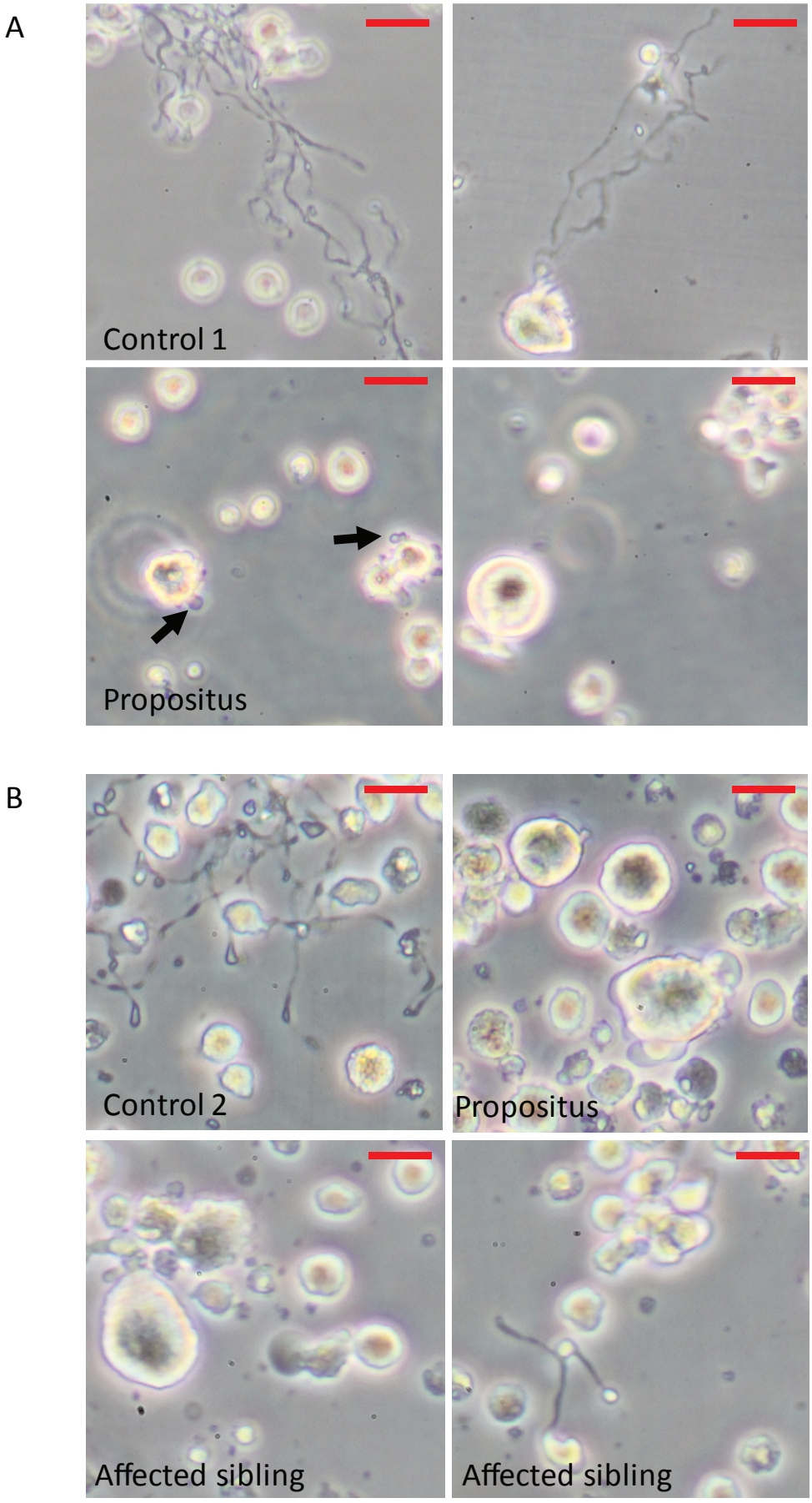

Supplemental Figure 9
Liquid megakaryocyte cultures show impaired proplatelet formation
(A) MK proplatelet formation was measured at day 11 of differentiation using bone marrow-derived CD34+ HSC from the propositus and controls. Propositus-derived MK were unusually large and displayed reduced proplatelet formation. (B) MK proplatelet formation was measured at day 12 of differentiation using peripheral blood derived CD34+ HSC from the propositus and affected sister. Again, MK from the patients were large and displayed membrane budding (arrows) but did not form normal proplatelets. Scale bars indicate 50 μm.

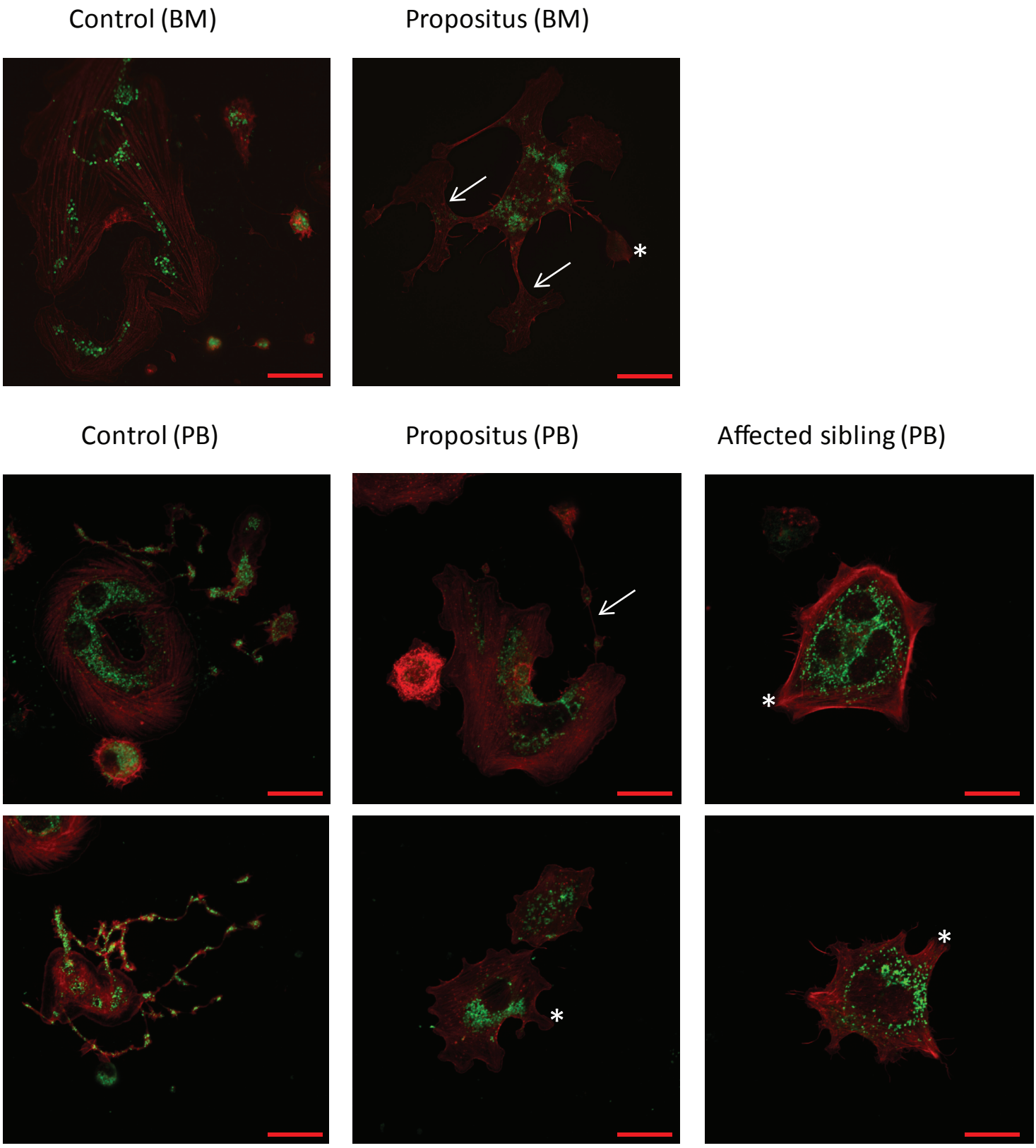

Supplemental Figure 10
Immunostaining of CD34+ stem cell-derived megakaryocytes confirm impaired proplatelet formation, and show abnormal cytoskeletal organisation
Megakaryocytes derived from bone marrow (BM) or peripheral blood (PB) were spread on fibrinogen and immunostained with antibodies against cytoskeletal marker F-actin (red) and δ-granule marker CD63 (green). MK for the propositus and his affected sibling showed irregular cytoskeletal structures that resembled filopodia (*). Proplatelet formation was infrequent and observed proplatelets demonstrated reduced δ-granule trafficking (arrow). Scale bars indicate 20μm.

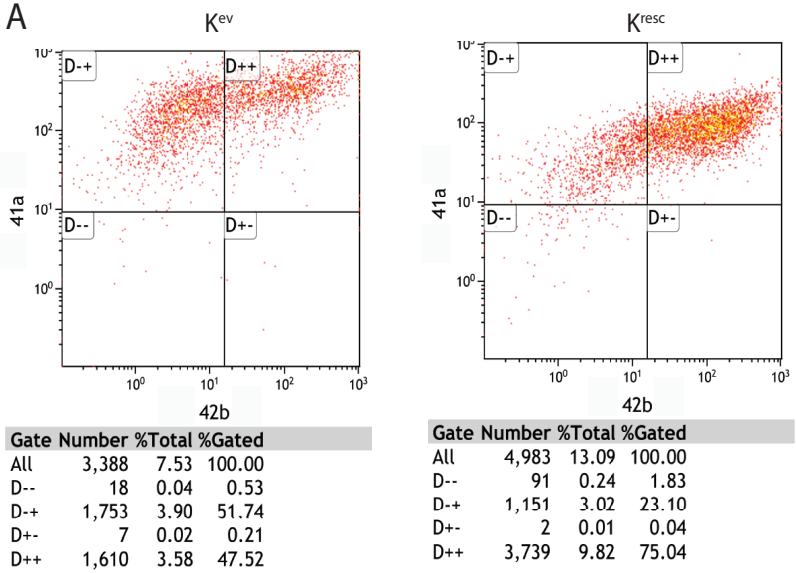

Gate	Number	%Total	%Gated
All	3,388	7.53	100.00
D--	18	0.04	0.53
D-+	1,753	3.90	51.74
D+-	7	0.02	0.21
D++	1,610	3.58	47.52

Gate	Number	%Total	%Gated
All	4,983	13.09	100.00
D--	91	0.24	1.83
D-+	1,151	3.02	23.10
D+-	2	0.01	0.04
D++	3,739	9.82	75.04

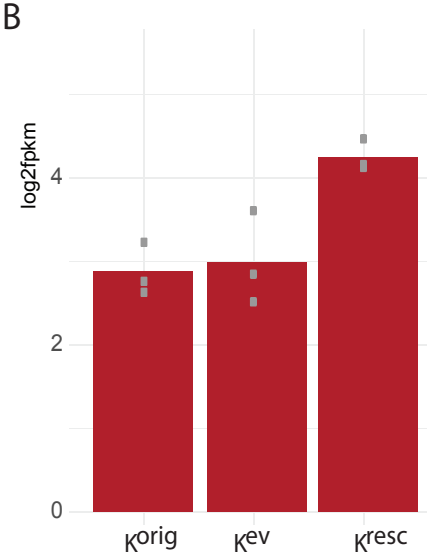

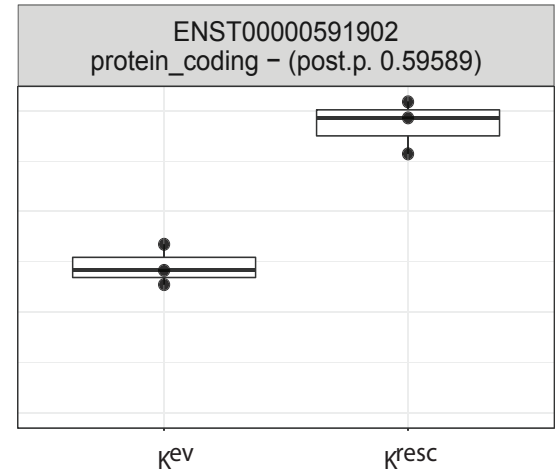

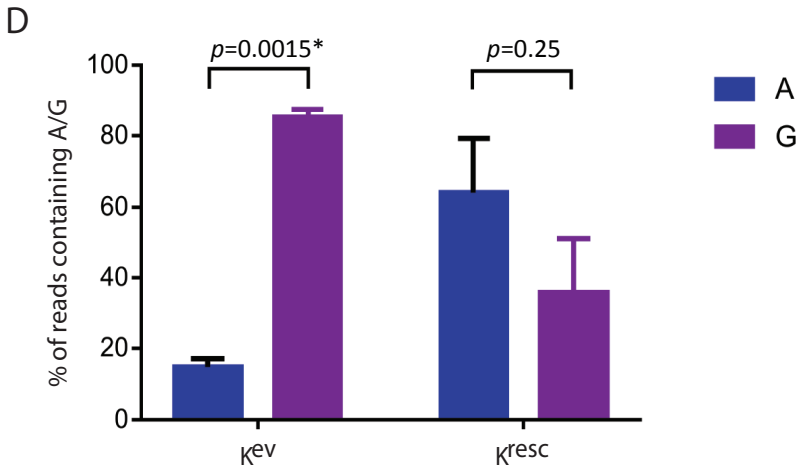

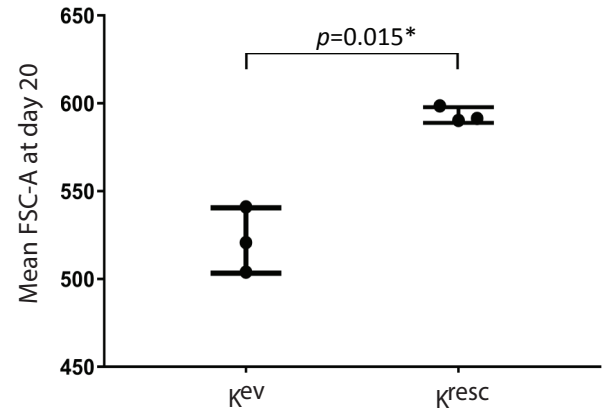

Supplemental Figure 11

Gene expression analysis by RNA-seq in K^{resc} and K^{ev} iMK is consistent with correction of the genetic defect, without significant overexpression

(A) iPSC from the propositus were transduced with lentiviral vectors containing the reference *KDSR* ORF (K^{resc}) or an inert control (K^{ev}), then reprogrammed to iMK. Single, viable cells were assessed by flow cytometry for markers of iMK at day 20 of forward programming. In both conditions the majority of cells were CD41+ and CD42+, in keeping with differentiation to iMK. (B) *KDSR* expression was assessed by RNA-seq. At the gene level there was no significant difference in normalised *KDSR* expression between propositus-derived iMK (K^{orig}), K^{ev} and K^{resc} iMK. (C) At the transcript level ENST00000591902 was differentially expressed and higher in K^{resc} iMK. This transcript corresponds to the *KDSR* sequence in the wild-type expression vector and is the transcript with the highest expression in MK.[8] A posterior probability of differential expression > 0·5 was considered significant. (D) K^{resc} iMK carried the reference allele at Chr18:61018270 G>A (p.Arg154Trp) (mean count G: 192 (84%), A: 36 (16%), $p = 0{\cdot}0015$ by paired, two-tailed *t*-test). K^{ev} iMK expression was consistent with heterozygosity (mean count G: 14 (33%), A: 29 (67%), $p = 0{\cdot}25$). Values plotted are mean number of transcripts and error bars show the standard deviation, across three independent experiments. (E) iMK were defined by flow cytometry as CD41+ viable, single cells and forward scatter area (FSC-A) was measured for each experimental replicate. The means and standard deviations of FSC-A are plotted for the three experimental replicates. At day 20 K^{resc} iMK were significantly larger than K^{ev} iMK ($p = 0{\cdot}015$ by paired, two-tailed *t*-test).

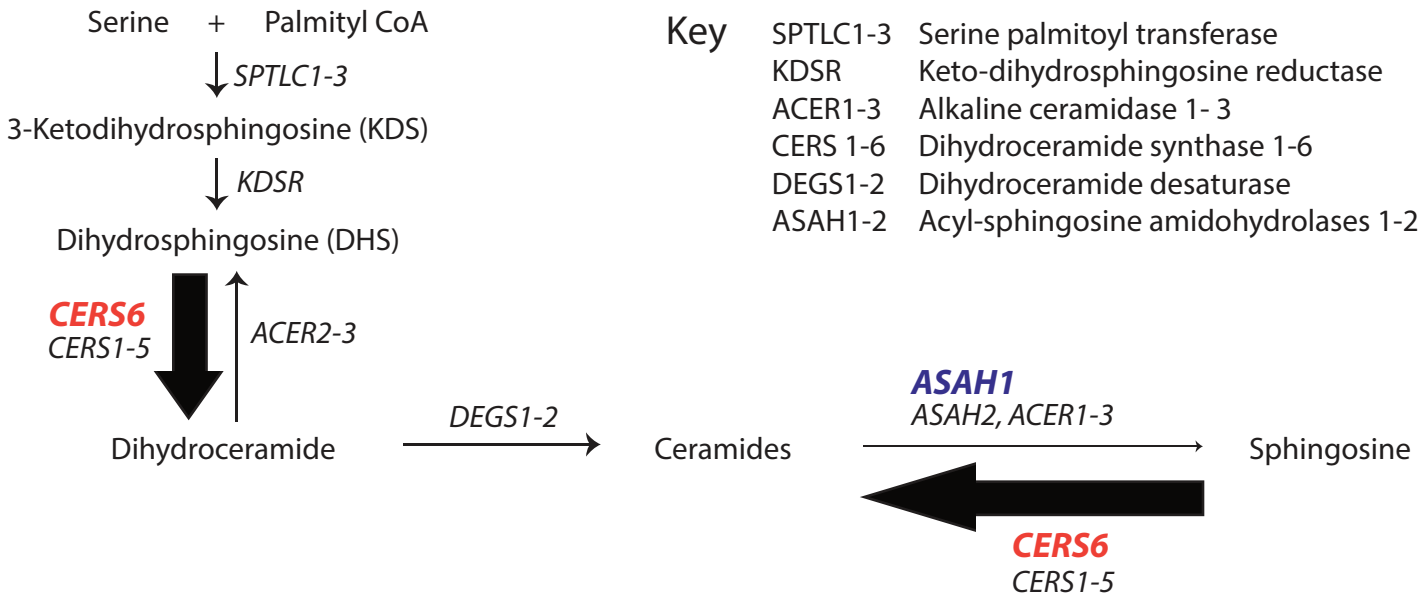

Supplemental Figure 12
Differential expression of ASAH1 and CERS6 between Kresc and Kev suggests that KDSR variants result in ceramide and sphingosine imbalance
Gene expression was assessed by RNA-seq. Using a posterior probability of differential expression > 0.5 for significance, only two of the sphingolipid enzymes listed in Figure 4A were significantly differentially expressed between K^{resc} and K^{ev}. ASAH1 (posterior probability = 0·61, estimated log fold change = -0·67) was down-regulated in the K^{ev} condition and CERS6 (posterior probability = 0·774, estimated log fold change = +0·70) was up-regulated in the K^{ev} condition. *ASAH1* and *CERS6* act in opposition to regulate the balance between ceramide and sphingosine. These findings are in keeping with the metabolic profile of higher sphingosine and lower ceramide in K^{resc} iMK compared with K^{ev} iMK shown in Figure 7.

Supplemental References

1. Westbury SK, Turro E, Greene D, Lentaigne C, Kelly AM, Bariana TK, et al. Human phenotype ontology annotation and cluster analysis to unravel genetic defects in 707 cases with unexplained bleeding and platelet disorders. Genome medicine. 2015; **7**(1): 36.
2. Schindelin J, Arganda-Carreras I, Frise E, Kaynig V, Longair M, Pietzsch T, et al. Fiji: an open-source platform for biological-image analysis. Nature methods. 2012; **9**(7): 676-82.
3. Westmoreland D, Shaw M, Grimes W, Metcalf DJ, Burden JJ, Gomez K, et al. Super-resolution microscopy as a potential approach to diagnosis of platelet granule disorders. J Thromb Haemost. 2016; **14**(4): 839-49.
4. Louwette S, Regal L, Wittevrongel C, Thys C, Vandeweeghde G, Decuyper E, et al. NPC1 defect results in abnormal platelet formation and function: studies in Niemann-Pick disease type C1 patients and zebrafish. Human molecular genetics. 2013; **22**(1): 61-73.
5. Freson K, Peeters K, De Vos R, Wittevrongel C, Thys C, Hoylaerts MF, et al. PACAP and its receptor VPAC1 regulate megakaryocyte maturation: therapeutic implications. Blood. 2008; **111**(4): 1885-93.
6. Turro E, Greene D, Wijgaerts A, Thys C, Lentaigne C, Bariana TK, et al. A dominant gain-of-function mutation in universal tyrosine kinase SRC causes thrombocytopenia, myelofibrosis, bleeding, and bone pathologies. Science translational medicine. 2016; **8**(328): 328ra30.
7. Heremans J, Garcia-Perez JE, Turro E, Schlenner SM, Casteels I, Collin R, et al. Abnormal differentiation of B cells and megakaryocytes in patients with Roifman syndrome. The Journal of allergy and clinical immunology. 2018.
8. Takahashi K, Tanabe K, Ohnuki M, Narita M, Ichisaka T, Tomoda K, et al. Induction of pluripotent stem cells from adult human fibroblasts by defined factors. Cell. 2007; **131**(5): 861-72.
9. Yu J, Vodyanik MA, Smuga-Otto K, Antosiewicz-Bourget J, Frane JL, Tian S, et al. Induced pluripotent stem cell lines derived from human somatic cells. Science. 2007; **318**(5858): 1917-20.
10. Moreau T, Evans AL, Vasquez L, Tijssen MR, Yan Y, Trotter MW, et al. Large-scale production of megakaryocytes from human pluripotent stem cells by chemically defined forward programming. Nature communications. 2016; **7**: 11208.
11. Dobin A, Davis CA, Schlesinger F, Drenkow J, Zaleski C, Jha S, et al. STAR: ultrafast universal RNA-seq aligner. Bioinformatics. 2013; **29**(1): 15-21.
12. Liao Y, Smyth GK, Shi W. featureCounts: an efficient general purpose program for assigning sequence reads to genomic features. Bioinformatics. 2014; **30**(7): 923-30.
13. Turro E, Astle WJ, Tavare S. Flexible analysis of RNA-seq data using mixed effects models. Bioinformatics. 2014; **30**(2): 180-8.
14. Turro E, Su SY, Goncalves A, Coin LJ, Richardson S, Lewin A. Haplotype and isoform specific expression estimation using multi-mapping RNA-seq reads. Genome biology. 2011; **12**(2): R13.
15. Chen L, Kostadima M, Martens JH, Canu G, Garcia SP, Turro E, et al. Transcriptional diversity during lineage commitment of human blood progenitors. Science. 2014; **345**(6204): 1251033.
16. Tani M, Sano T, Ito M, Igarashi Y. Mechanisms of sphingosine and sphingosine 1-phosphate generation in human platelets. Journal of lipid research. 2005; **46**(11): 2458-67.